CrystEngComm

Dynamic Article Links

Cite this: *CrystEngComm*, 2011, **13**, 3451

www.rsc.org/crystengcomm

PAPER

Botryoidal growth of crystalline ZnO nanoparticles on a forest of single-walled carbon nanotubes by atomic layer deposition

Yo-Sep Min,*[a] Il Ha Lee,[b] Young Hee Lee[b] and Cheol Seong Hwang[c]

Received 23rd November 2010, Accepted 12th February 2011
DOI: 10.1039/c0ce00875c

Atomic layer deposition (ALD) is a type of chemical vapor deposition method specially modified to grow thin films *via* a so called self-limiting growth mechanism. In spite of its excellent conformality due to inherent layer-by-layer growth behavior, the utilization of ALD is restricted mainly to the growth of thin films. In this article we demonstrate that ZnO nanoparticles can be grown with a botryoidal appearance by ALD using a forest of single-walled carbon nanotubes as the substrate, which only has a sparse amount of reactive sites for precursor chemisorption. The nanoparticles are fairly spherical and single crystalline with a wurtzite crystalline structure. The growth rate of the nanoparticles is roughly estimated to be ~2.8 Å cycle^{-1} which is around twice the growth rate of a conformal film on a flat substrate. The size of the nanoparticles is considerably uniform with a standard deviation of ~18%.

Introduction

Since atomic layer deposition (ALD) was introduced in the late 1970s, ALD has been intensively studied to deposit various thin films for dielectric, metallic and luminescent applications.[1–4] In ALD, an appropriate precursor vapor and a reaction gas are alternately pulsed onto a substrate that is maintained at a temperature low enough to avoid the spontaneous thermal decomposition of the precursor. Between each alternating pulse, the reaction chamber is purged with an inert gas. The cycle of an ALD process generally consists of an aggregate of these steps, usually being in the form of precursor exposure–purge–reaction gas exposure–and purge again. Consequently, film growth occurs by chemical adsorption (*i.e.*, chemisorption) of the gaseous molecules (*i.e.*, precursor vapor or reactant gas) onto the reactive functional groups on the surface (*e.g.*, hydroxyl groups or chemisorbed organometallic groups).

Due to the inherent nature of ALD, which depends on the number of chemisorption sites, once all vacant sites become saturated by adsorbate molecules and a monolayer is formed (practically, a sub-monolayer is formed because of the bulkiness of the adsorbate molecules), the leftover precursor or reactant gas molecules cannot chemically adsorb onto the substrate. This is the origin of the self-limiting *layer-by-layer* growth in ALD.[2]

Recently, several research groups have tried to use ALD to prepare nano-tubular materials by using the characteristic conformal growth behavior of ALD on various templates such as carbon nanotubes (CNTs) or anodic aluminium oxide.[5–11] Furthermore, the attempt to grow nanoparticles by ALD has also been under rigorous investigation for catalyst applications.[12–14] Christensen *et al.* reported that the ALD of noble metals, such as Pt and Ru, generates nanoparticles during the initial stage of growth due to the coalescence of metallic atoms.[12–14] However studies on the nanoparticle growth of non-noble metals by ALD are still rare because ALD generally gives a conformal film under conditions where adsorption sites are uniformly distributed with a high density (Fig. 1a).

On the other hand, if there are no reactive adsorption sites on the surface for the ALD reaction to occur, thin films cannot be grown by this method. For example the surface of a CNT, which consists of sp^2 carbons, is quite inert to most precursors or reaction gases. Therefore it is extremely difficult to deposit conformal thin films on CNTs using ALD. Gordon and Farmer reported that the conformal coating of a single-walled carbon nanotube (SWCNT) by ALD could be realized only after the covalent or non-covalent functionalization of the nanotube wall because of the absence of reactive sites in these materials.[15,16] However, it should be noted that the growth of nanotubes is inevitably accompanied by defect and/or impurity incorporation.[17] These defective sites can act as reactive adsorption sites, and indeed George *et al.* reported that the ALD of Al_2O_3 on multi-walled CNTs formed nanoparticles due to the presence of defects or inadvertent chemical functionalization on the nanotube surface.[18] We also reported that ZnO nanoparticles could be

[a]*Department of Chemical Engineering, Konkuk University, Seoul, 143-701, Korea. E-mail: ysmin@konkuk.ac.kr; Fax: +82 2 458 3504; Tel: +82 2 458 7626*
[b]*BK21 Physics Division, Department of Energy Science, Center for Nanotube and Nanostructured Composites, Sungkyunkwan Advanced Institute of Nanotechnology, Sungkyunkwan University, Suwon, 440-746, Korea*
[c]*WCU Hybrid Materials Program, Department of Materials Science & Engineering and Inter-university Semiconductor Research Center, Seoul National University, Seoul, 151-744, Korea*

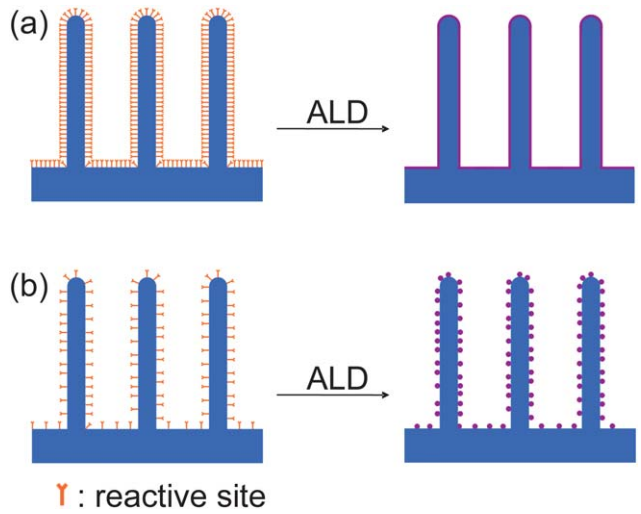

Fig. 1 (a) A typical conformal film grown by ALD on a substrate with a high reactive site density and (b) nanoparticles grown by ALD on a substrate with only a sparse amount of reactive sites.

selectively grown by ALD on defects or impurities on the wall of a SWCNT, which resulted in the significant elongation of the field emission lifetime of the nanotube.[19] In this work, it was conjectured that ALD on a substrate with only a sparse amount of reactive sites would give nanoparticles instead of a conformal film (Fig. 1b).

Meanwhile the authors demonstrated that a highly pure and crystalline SWCNT network could be grown at 450 °C by water plasma chemical vapor deposition (CVD).[20,21] By choosing an appropriate catalyst and precisely controlling the process, a forest of vertically grown SWCNTs can also be obtained at the same low temperature.[22]

The SWCNT forest vertically grown by the water plasma CVD was used as the substrate with only a sparse amount of reactive sites for ALD. Here, it is reported that ALD can be utilized to grow ZnO nanoparticles with a botryoidal appearance. The nanoparticles are fairly spherical and single crystalline with a wurtzite crystalline structure. The growth rate of the nanoparticles is around 2.8 Å cycle^{-1} which is around twice the growth rate of a conformal film on a flat substrate. The sizes of the nanoparticles are considerably uniform with a standard deviation of ~18%.

Experimental

The catalyst for the growth of the SWCNT forest was formed on a SiO_2 (200 nm)/Si wafer by following the procedures below: an Al thin film (10 nm) was deposited on the substrate by thermal evaporation, and then oxidized at 700 °C in air. Then an ultrathin Fe film (0.5 nm) was e-beam evaporated and subsequently thermally oxidized at 600 °C for 10 min in air. The SWCNT forest was then grown at 450 °C for 20 min on the catalyst substrate. The growth conditions for the SWCNT forest were the same as the nanotube network except for the preparation method of a catalyst substrate (see ref. 21 and 22 for details on the process conditions).

The ALD of ZnO was performed on the SWCNT forest at 250 °C using diethylzinc (DEZ) and water which were both vaporized at room temperature and delivered to the ALD reactor without any carrier gas. The exposure time for both DEZ and water was 10 s. After each exposure step, the reaction chamber was purged with Ar (1600 sccm) for 30 s. The ALD sequence was repeated for 40 cycles.

Results and discussion

The cross-sectional scanning electron microscopic (SEM) image in Fig. 2a shows the forest of SWCNTs grown on a SiO_2 (200 nm)/Si wafer for 20 min at 450 °C by water plasma CVD. Prior to the growth of the SWCNT forest, an ultrathin iron oxide film was formed on the substrate as a catalytic layer for the nanotube growth. The SWCNTs are densely packed and are well-aligned with a vertical orientation to the substrate. Fig. 2b and c show magnified images of the top and middle regions of a 20 min-grown forest, respectively. According to the Raman spectra and high resolution transmission electron microscopic (TEM) images of the forest (data in ref. 22), most of the nanotubes were single-walled and bundled.[22] However, the D-band (disorder-induced mode) to G-band (tangential stretching mode) intensity ratio in the Raman spectra was 2–5 times larger for the SWCNT forest (0.1–0.2) compared to that (0.04–0.05) of the SWCNT network.[21,22] This reveals that nanotubes in the forest have much more defects and/or impurities than the SWCNT network. Because a non-negligible amount of water is supplied to the reactor during the growth of the SWCNTs, it is expected that the nanotubes have oxygen- or hydroxyl-containing defects and/or impurities on the wall, which may act as reactive adsorption sites for ALD.[23] However in comparison with typical oxide substrates, the density of reactive sites in a SWCNT forest is still far too low to form a conformal film (*vide infra*).

The ALD of ZnO was performed on the SWCNT forest at 250 °C using DEZ as the precursor and water vapor as the reaction gas for hydrolysis. For a flat substrate, the exposure or purging times required for the self-limiting growth to dominate are generally shorter than several seconds.[24] However our

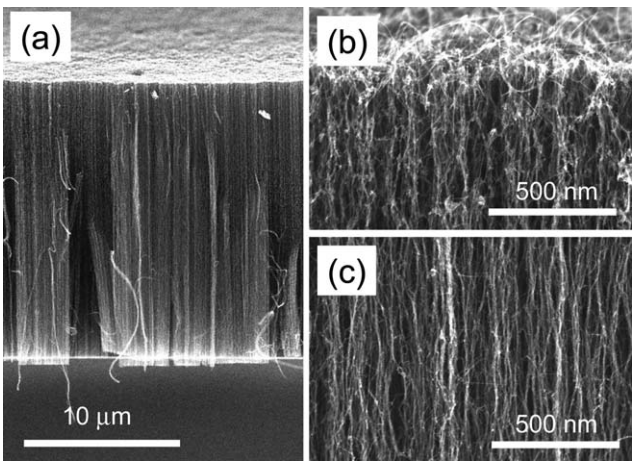

Fig. 2 (a) Cross-sectional SEM image of a SWCNT forest grown at 450 °C for 20 min. (b and c) Magnified images of the top and middle regions in Fig. 2a, respectively.

substrate has a much larger surface area due to the presence of the SWCNT forest. Furthermore the transport path for the precursors and gaseous byproducts is much longer and tortuous. Thus the exposure (10 s) and purging (30 s) times were extended to much longer times in this experiment.

Fig. 3 shows cross-sectional SEM images of the SWCNT forest on which ZnO ALD was performed for 40 cycles. As anticipated, spherical nanoparticles were grown instead of a conformal film. Generally, when growing conformal oxide films by ALD, the areal density of hydroxyl groups, which are typical reactive sites for oxide ALD, is several OH groups per nm^2. For example the areal density of OH groups on alumina is 8–9 OH nm^{-2}.[25] Therefore the fact that nanoparticles are grown by ALD reveals that although there is a considerable amount of reactive defect and/or impurities on the wall of the nanotubes, the areal density of them is much smaller than several sites per nm^2.

Interestingly, the nanoparticles grown on the SWCNT forest show a botryoidal appearance resembling a bunch of grapes, which is believed to come from the considerable amount of reactive sites on the SWCNTs. Besides, in spite of the extremely crowded nature of the SWCNTs in the forest, nanoparticles were grown everywhere from the top to the bottom regions of the forest. It reveals that the exposure and purging times of DEZ and water were long enough to guarantee ALD chemistry.

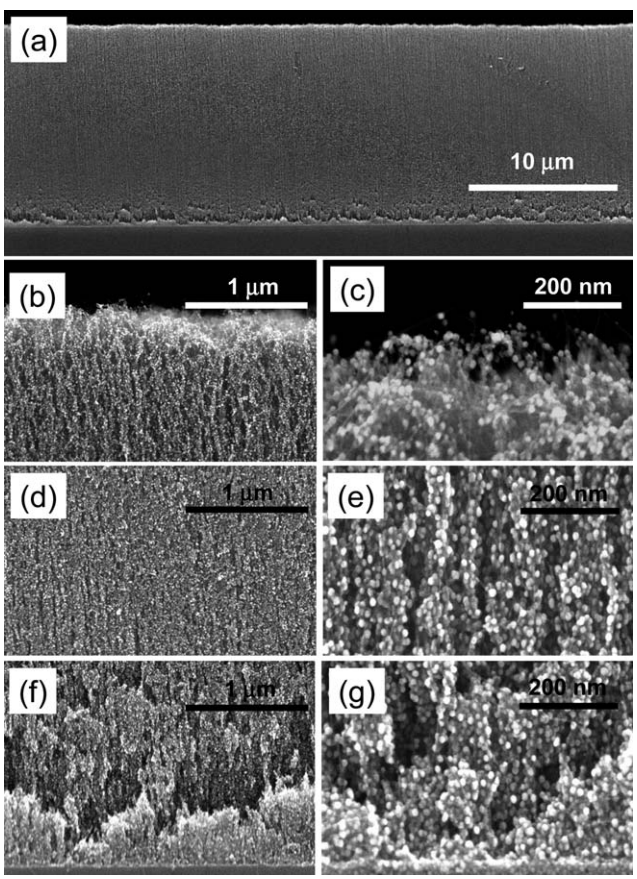

Fig. 3 (a) Cross-sectional SEM image of the SWCNT forest with ALD-grown ZnO nanoparticles. (b and c), (d and e), and (f and g) Magnified images of the top, middle and bottom regions in Fig. 3a, respectively.

However the population of the nanoparticles is slightly denser near the bottom than in regions near to the top. The different populations of nanoparticles in the top and bottom regions of nanotubes may originate from the initial distribution difference of defects and/or impurities that are reactive to precursors. As nanotubes grow, the activity of catalysts generally deteriorates. This results in a higher defect and/or impurity density in the bottom region because our SWCNT forest is grown *via* the root-growth mechanism.[22,26]

According to previous studies, ALD gives a conformal thin film on highly defective nanotubes,[5,6,27] but only a few nanoparticles are formed on highly crystalline nanotubes.[15,18,19] The number of nanoparticles formed per unit length of a nanotube is strongly dependent on its defect density. Recently, Kern *et al.* reported that Se nanoparticles can be site-selectively grown on oxygen-containing defects in SWCNTs by exposing them to H_2Se.[23] Their method could be utilized to titrate chemical defects and reveal defect locations in a single tube.

For further characterization of the ZnO nanoparticles by TEM and energy dispersive X-ray spectroscopy (EDS), the SWCNT forest with nanoparticles was detached from the substrate and dissolved in acetone. Subsequently a drop of the solution was placed and dried on a TEM grid. As can be seen in the inset of Fig. 4a, the nanoparticles were identified to be ZnO with Zn and O peaks in the EDS spectrum. Of course, a strong carbon peak from the SWCNTs is also observed. The Cu signal is from the TEM grid. Fig. 4a shows a low resolution TEM image of the ZnO nanoparticles grown by ALD. The nanoparticles are fairly spherical and monodisperse with a narrow size distribution

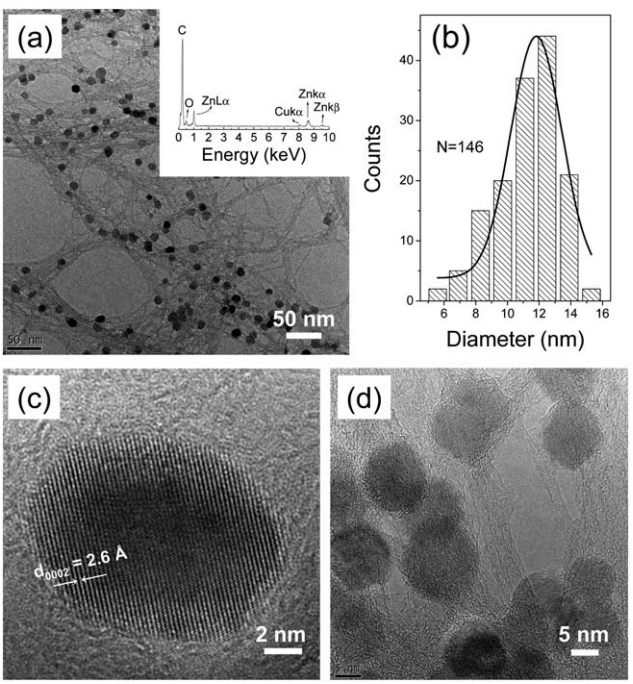

Fig. 4 (a) TEM image of the spherical ZnO nanoparticles grown on the SWCNT forest. The inset shows an EDS spectrum of the SWCNT forest with ZnO Nanoparticles. (b) The histogram of the diameters of the ZnO nanoparticles determined from Fig. 4a. (c and d) High resolution TEM images of the nanoparticles.

as shown in Fig. 4b. The average diameter of 146 nanoparticles measured from the TEM image was around 11.3 nm with a standard deviation of ±2.06 nm (~18%). This deviation may originate from the different incubation times experienced on dissimilar adsorption sites. The later-nucleated sites should experience fewer ALD cycles and consequently produce smaller nanoparticles.[18] From the average diameter of the nanoparticles grown for 40 cycles, the growth rate of the nanoparticles by ALD is roughly estimated to be ~2.8 Å cycle^{-1} which is around twice the growth rate of a conformal film on a flat substrate (1.3–1.4 Å cycle^{-1}) at 250 °C.[24] It should be noted that during the nanoparticle growth, ZnO grows spherically with an increasing radius as the ALD cycles are repeated.

According to the ZnO ALD on flat substrates, since ZnO is easily crystallized during ALD, polycrystalline thin films are obtained even at 150 °C, and films grown at temperatures over 300 °C show a ⟨002⟩ preferred orientation.[24] Even more dramatically, the as-grown nanoparticles on the SWCNT forest were singe-crystalline as shown in Fig. 4c and d. The lattice fringes of the (0002) planes with a *d*-spacing of 2.6 Å, which corresponds to the wurtzite crystalline structure of ZnO, are clearly seen in Fig. 4c. The single-crystalline structure reveals the high possibility that ZnO nucleates mainly on a single defect site for each nanoparticle. If several defect sites contributed to the nucleation and the growth of ZnO, the crystalline structure of the nanoparticles should be polycrystalline.

Recently, nanostructured ZnO has been intensively studied for potential applications in hydrogen storage, sensors and solar cells.[28–30] ZnO is also utilized as a catalyst in the steam reforming of methanol.[31] The common feature of these applications is that their properties can be improved when the specific surface area of ZnO is increased. In this point of view, our botryoidal ZnO nanoparticles on SWCNTs are expected to be a promising candidate for commercial use in these applications.

Conclusions

Although ALD is a well-known method for the conformal growth of thin films *via* the self-limiting growth mechanism, it was found that crystalline nanoparticles with a fairly uniform size distribution could also be grown by using a SWCNT forest as the ALD substrate which has only a sparse amount of reactive sites for the ALD chemistry. The ALD approach for the growth of botryoidal nanoparticles on a SWCNT forest can be utilized in various applications such as catalysis, gas storage, sensors and solar cells which require a large specific surface area.

Acknowledgements

This research was supported by the National Research Foundation (NRF) of Korea funded by the Ministry of Education, Science and Technology (MEST) of Korea (2009-0077062 and 2009-0081967), and also partially supported by SFC. Y.H.L. acknowledges the financial support from star-faculty program, World Class University (WCU) program (2008-000-10029-0), and the International Research & Development Program (2010-00429) of NRF funded by MEST. C.S.H. acknowledges the support from WCU program through the Korea Science and Engineering Foundation funded by MEST (R31-2008-000-10075-0).

References

1 T. Suntola and J. Antson, *US Pat.,* 4,058,430, 1977.
2 T. Suntola, in *Handbook of Crystal Growth*, ed. D. T. J. Hurle, Elsevier, Amsterdam, 1994; vol. 3, ch. 14A.
3 M. Ritala and M. Leskela, in *Handbook of Thin Film Materials*, ed. H. S. Nalwa, Academic Press, San Diego, 2002, vol. 1, ch. 2.
4 Y. S. Min, Y. J. Cho and C. S. Hwang, *Chem. Mater.*, 2005, **17**, 626.
5 Y. S. Min, E. J. Bae, K. S. Jeong, Y. J. Cho, J. H. Lee and W. B. Choi, *Adv. Mater.*, 2003, **15**, 1019.
6 J. S. Lee, B. Min, K. Cho, S. Kim, J. Park, Y. T. Lee, N. S. Kim, M. S. Lee, S. O. Park and J. T. Moon, *J. Cryst. Growth*, 2003, **254**, 443.
7 H. Shin, D. K. Jeong, J. Lee, M. M. Sung and J. Kim, *Adv. Mater.*, 2004, **16**, 1197.
8 M. S. Sander, M. J. Cote, W. Gu, B. M. Kile and C. P. Tripp, *Adv. Mater.*, 2004, **16**, 2052.
9 R. H. A. Ras, M. Kemell, J. D. Wit, M. Ritala, G. T. Brinke, M. Leskela and O. Ikkala, *Adv. Mater.*, 2007, **19**, 102.
10 J. Bachmann, J. Jing, M. Knez, S. Barth, H. Shen, S. Mathur, U. Gosele and K. Nielsch, *J. Am. Chem. Soc.*, 2007, **129**, 9554.
11 M. Knez, K. Nielsch and L. Niinistoe, *Adv. Mater.*, 2007, **19**, 3425.
12 S. T. Christensen, J. W. Elam, B. Lee, Z. Feng, M. J. Bedzyk and M. C. Hersam, *Chem. Mater.*, 2009, **21**, 516.
13 S. T. Christensen, J. W. Elam, F. A. Rabuffetti, Q. Ma, S. J. Weigand, B. Lee, S. Seifert, P. C. Stair, K. P. Poeppelmeier, M. C. Hersam and M. J. Bedzyk, *Small*, 2009, **5**, 750.
14 S. T. Christensen, H. Feng, J. L. Libera, N. Guo, J. T. Miller, P. C. Stair and J. W. Elam, *Nano Lett.*, 2010, **10**, 3047.
15 D. B. Farmer and R. G. Gordon, *Electrochem. Solid-State Lett.*, 2005, **8**, G89.
16 D. B. Farmer and R. G. Gordon, *Nano Lett.*, 2006, **6**, 699.
17 Y. S. Min, E. J. Bae and W. Park, *J. Am. Chem. Soc.*, 2005, **127**, 8300.
18 A. S. Cavanagh, C. A. Wilson, A. W. Weimer and S. M. George, *Nanotechnology*, 2009, **20**, 255602.
19 Y. S. Min, E. J. Bae, J. Song, J. B. Park, N. J. Park, W. Park and C. S. Hwang, *Appl. Phys. Lett.*, 2007, **90**, 263104.
20 E. J. Bae, Y. S. Min, J. H. Ko, D. Kang and W. Park, *Chem. Mater.*, 2005, **17**, 5141.
21 Y. S. Min, E. J. Bae, B. S. Oh, D. Kang and W. Park, *J. Am. Chem. Soc.*, 2005, **127**, 12498.
22 I. H. Lee, J. Im, U. J. Kim, E. J. Bae, K. K. Kim, E. H. Lee, Y. H. Lee, S. H. Hong and Y. S. Min, *Bull. Korean Chem. Soc.*, 2010, **31**, 2819.
23 Y. Fan, M. Burghard and K. Kern, *Adv. Mater.*, 2002, **14**, 130.
24 Y. S. Min, C. J. An, S. K. Kim, J. Song and C. S. Hwang, *Bull. Korean Chem. Soc.*, 2010, **31**, 2503.
25 R. L. Puurunen, M. Lindblad and A. O. I. Krause, *Phys. Chem. Chem. Phys.*, 2001, **3**, 1093.
26 J. Gavillet, A. Loiseau, C. Journet, F. Willaime, F. Ducastelle and J. C. Charlier, *Phys. Rev. Lett.*, 2001, **87**, 275504.
27 C. F. Herrmann, F. H. Fabreguette, D. S. Finch, R. Geiss and S. M. George, *Appl. Phys. Lett.*, 2005, **87**, 123110.
28 Q. Wan, C. L. Lin, X. B. Xu and T. H. Wang, *Appl. Phys. Lett.*, 2004, **84**, 124.
29 H. T. Wang, B. S. Kang, F. Ren, L. C. Tien, P. W. Sadik, D. P. Norton, S. J. Pearton and J. Lin, *Appl. Phys. Lett.*, 2005, **86**, 243503.
30 C. Y. Jiang, X. W. Sun, G. Q. Lo, D. L. Kwong and J. X. Wang, *Appl. Phys. Lett.*, 2007, **90**, 263501.
31 M. M. Gunter, T. Ressler, R. E. Jentoft and B. Bems, *J. Catal.*, 2001, **203**, 133.

